

LOCAL HEATING AND CURING OF CARBON NANOCOMPOSITE ADHESIVES  
USING RADIO FREQUENCIES

A Thesis

by

JACOB THOMAS GRUENER

Submitted to the Office of Graduate and Professional Studies of  
Texas A&M University  
in partial fulfillment of the requirements for the degree of

MASTER OF SCIENCE

Chair of Committee,	Micah Green
Committee Members,	Yossef Elabd
	Mohammad Naraghi
Head of Department,	M. Nazmul Karim

May 2019

Major Subject: Chemical Engineering

Copyright 2019 Jacob Gruener

## ABSTRACT

In this thesis, the phenomenon of carbon nanoparticles producing a strong, rapid heating response in the presence of a radio-frequency electromagnetic field is explored, and this extremely selective heating property is used to cure nanocomposite thermoset adhesives without harming the surrounding plastic components. By dispersing carbon black nanoparticles into the adhesive matrix, the heat needed to cure the adhesive can be supplied by the RF-responsive nanoparticles, generating heat volumetrically inside the adhesive. Because this heat is selectively generated only in the adhesive, the substrates being bonded together can be kept at a temperature lower than the desired curing temperature of the adhesive. For example, substrate temperatures as low as 52.8°C were observed while the adhesive was curing at 85°C, in stark contrast to the higher substrate temperatures seen when curing adhesive using conventional heating methods, such as an IR lamp. The degree of cure is confirmed by mechanical tests: lap shear strengths of these RF-cured adhesive joints were 478.2 psi on average, well above the recommended green strength of 1 MPa (145 psi). These results demonstrate the viability of this technology and pave the way to expand its application toward industrial manufacturing, particularly in the automotive sector where thermoset adhesives are ubiquitous.

## ACKNOWLEDGEMENTS

I would like to heartily thank Dr. Micah Green for being an incredible advisor these two years. As a mentor, he has been very energetic and motivating, but also very patient and understanding. Despite the numerous other researchers and projects he manages, he was always fully present for me when I encountered difficulties, and was more than willing to help brainstorm potential solutions and new directions. I could not have accomplished what I have for this thesis without him.

I would also like to thank Dr. Yossef Elabd, and Dr. Mohammad Naraghi, for joining my committee and advising me along the way.

I would like to thank the rest of the Green Group, for accepting me into their ranks and showing me the ropes in the lab. In particular, I'd like to thank Brandon Sweeney, for teaching me about our prior work with microwaves and RF, and Aniruddh Vashisth, for providing help and insight in this project.

I would like to thank each and every friend I made at Texas A&M, but this section is supposed to be short, so I'll just thank you all at once. I'm beyond grateful to have made had such great friends with which to share all the grinds of college.

Lastly, I'd like to thank my parents. You both instilled in me an appreciation for knowledge and the internal motivation to learn. I could never have made it to where I am today without all of your love and support. Thank you for always pushing me to be a better person, in all things. I love you both.

## CONTRIBUTORS AND FUNDING SOURCES

This thesis was supervised and reviewed by a committee of professors, including Dr. Micah Green (advisor) and Dr. Yossef Elabd of the Department of Chemical Engineering and Dr. Mohammad Naraghi of the Department of Aerospace Engineering.

The SEM imaging discussed in this thesis was performed by Aniruddh Vashisth. Materials for sample preparation, temperature and strength data for the IR lamp heating process, and additional knowledge and guidance were all provided by Tyler Auvil and Dan Sophiea, from the Dow Chemical Company.

The work detailed in this thesis was funded by The Dow Chemical Company.

## TABLE OF CONTENTS

	Page
ABSTRACT .....	ii
ACKNOWLEDGEMENTS .....	iii
CONTRIBUTORS AND FUNDING SOURCES.....	iv
TABLE OF CONTENTS .....	v
LIST OF FIGURES .....	vi
LIST OF TABLES .....	viii
1. INTRODUCTION.....	1
1.1. Thermosets .....	1
1.2. Fillers in thermosets .....	2
2. BACKGROUND.....	4
2.1. Carbon nanoparticles as microwave/RF susceptors .....	4
2.2. The need for localized heating in adhesive bonding .....	11
2.3. New approach: Application of carbon nanoparticles as local heaters.....	13
3. EXPERIMENTAL METHODS AND RESULTS .....	15
3.1. Materials and Procedures .....	15
3.1.1. Materials .....	15
3.1.2. Procedures .....	15
3.2. Results .....	19
3.2.1. Design of the RF applicator.....	19
3.2.2. Thermal data: Adhesive and substrates .....	24
3.2.3. Mechanical data: Lap shear testing and shear strength .....	27
3.2.4. SEM imaging: Toughening mechanism & adhesive weakening near carbon black .....	31
3.2.5. Direct contact heating on carbon fiber .....	33
4. CONCLUSION .....	35
4.1. Conclusion.....	35
REFERENCES .....	38

## LIST OF FIGURES

	Page
Figure 1 - A) 3D-printed parts using carbon nanotube ink-coated printer filament and B) the effect of microwave heating at the interfaces between print layers (reproduced from Sweeney <i>et al.</i> , 2017) .....	7
Figure 2 - Heating response of MWCNT/PLA composite films of varying wt% MWCNTs to various radio frequencies (reproduced from Sweeney <i>et al.</i> , 2018) .....	8
Figure 3 - Heating of a carbon nanotube/epoxy composite using RF energy (adapted from Sweeney <i>et al.</i> , 2018).....	9
Figure 4 - 1) Side-view schematic detailing the experimental setup of the sample and the RF applicator, and 2) Side-view thermal image of a sample being subjected to RF energy at 116 MHz .....	17
Figure 5 – COMSOL model of the fringing electric field in the volume above a coplanar plate capacitor .....	19
Figure 6 - Excerpt from Figure 2 of Sweeney <i>et al.</i> (2018), showing (C) the geometry and expected heating profile of the interdigitated capacitor, and (F) a FLIR thermal image of a composite MWCNT/PLA thin film being heated by this capacitor.....	21
Figure 7 - Top view of the thermal response of ~2 mm of adhesive on top of a TPO coupon, after 5 minutes of RF exposure (32 W, 116 MHz) using applicators with 1) 13 mm spacing (½ inch), and 2) 3 mm spacing .....	22
Figure 8 - Temperature profiles of samples during heating using 1) an IR lamp (data captured using thermocouples) and 2) RF heating (data captured using FLIR camera) .....	25
Figure 9 - The areas over which mean temperature was calculated are shown for LGFPP (green) and TPO (blue).....	26
Figure 10 - Stress-strain curves for samples cured at 85°C for 2 minutes, with a sample cured for at 85°C for 10 minutes for comparison .....	28
Figure 11 - Stress vs. displacement curves for lap joint samples using 1) the IR bonder (heat for 3 minutes, let stand for specified time) and 2) RF heating (heat for specified time, let stand for 30 minutes).....	30

Figure 12 - Diagrams showing 1) how carbon black nanoparticles deflect cracks into the surrounding matrix, and 2) how dispersions of nanoparticles provide extra toughness by lengthening the path of the crack, increasing the total energy required to propagate it .....	31
Figure 13 - SEM images of adhesive fracture surface post shear testing, showing layered failure planes (left) and the semi-rough surface (right) .....	32
Figure 14 - Thermal data for the carbon fiber/epoxy composite coupon and carbon black-loaded adhesive during cure .....	34

## LIST OF TABLES

	Page
Table 1 - Loss tangent measurements for various carbon allotropes at 2.45 GHz.....	5
Table 2 - Heating response of 1 mg samples of carbon to 1 second of microwave radiation (2.45 GHz, 30 W) (adapted from Irin <i>et al.</i> , 2012) .....	6



## 1. INTRODUCTION

### 1.1. Thermosets

Most commercially-produced polymers fall into one of two categories: thermoplastic or thermoset. Most people are more familiar with thermoplastics: they comprise all of the numbered recycling plastics 1 through 6, including big names like polyethylene and poly(vinyl chloride) (PVC), and they accounted for around 88% of all plastics produced in 2015<sup>1</sup>. However, thermosets also play an important role both industrially and commercially. They have a variety of uses, from load-bearing structural components, to smooth-finish protective films and sealants, to high-strength bonding adhesives.

The characteristic that defines a polymer as a thermoset is that it is irreversibly hardened, or “cured,” at high temperatures. These high temperatures initiate chemical reactions that create cross-links between the long polymer chains, forming a complex network of covalently bonded segments. These cross-links give thermosets great strength, making them desirable for load-bearing applications. Because their strength is derived from the chemical properties obtained via irreversible reaction, thermosets do not lose shape or strength upon being reheated. For this reason, they fare better in high-temperature applications than thermoplastics and are often used as hard outer laminates and protective sealants.

Before being cured, however, most thermosets exist in more pliable forms, such as liquid solutions, putty-like suspensions, or rubbery solids. In these phases, thermosets can

be easily processed, being molded into a desired shape, or spread over a surface; then, by heating the thermoset and initiating curing, this custom-molded shape can be irreversibly solidified. This property makes thermosets ideal candidates for adhesives. When heated up, the thermoset forms crosslinks between itself and the surfaces on which it's applied, forming a strong joint between the parts without the need to damage any facet of their structural integrity, as with rivets or welding. Adhesives are becoming a more popular choice for manufacturers in a variety of industries for many different bonding applications, including everything from beverage labels to automotive parts.

## **1.2. Fillers in thermosets**

To broaden the scope of potential applications for many thermosets, people will often add fillers. The addition of fillers can create different formulations of the same base polymer, leading in some cases to drastically improved material properties. Some common properties that can be adjusted using fillers are electrical and thermal conductivities, stiffness, fracture toughness, tensile strength, UV susceptibility, and color/pigmentation. Most fillers are either macro-scale particulates, as in the case of calcium carbonate or kaolin clay, or high aspect-ratio fibers, such as glass or carbon fibers.

In recent years, people have begun to investigate the use of nano-fillers in thermosets. Nanoparticles make better fillers for composite materials for one main reason: they have much higher specific surface areas. Since volume scales with the cube of particle diameter, and surface area scales with the square of diameter, nanoparticles expose much more surface area per volume. This provides a number of benefits, including lower

percolation thresholds<sup>2</sup>, shorter distances between filler particles<sup>2,3</sup>, and higher reinforcement strengths<sup>4</sup>. With nanoparticles, using a lower weight percentage of filler can result in similar or better characteristic improvements than can be achieved with macro-scale fillers.

In this thesis, we focus on a largely unexplored use of nano-fillers: localized heating. Carbon-based nanoparticles, such as carbon nanotubes and carbon black, have been proven to respond strongly in the presence of microwave- and radio-frequency (RF) radiation, and rapidly generate heat<sup>5-11</sup>. When embedded in a thermosetting adhesive matrix, these nanotubes can be subjected to RF radiation to generate heat from within the adhesive, initiating the curing reaction without the need for external heat transfer. This is a promising technology, with a variety of potential applications in joining and welding large metallic or plastic parts together. The application that will be investigated in this thesis is the ability to selectively heat the target adhesive while maintaining relatively cooler temperatures for its substrates.

## 2. BACKGROUND\*

### 2.1. Carbon nanoparticles as microwave/RF susceptors

Carbon nanomaterials have a well-documented history of strong thermal responses to electromagnetic (EM) fields. They have been investigated both for their ability to heat selectively when exposed to microwave radiation<sup>8,9</sup> and their ability to impart EMI-shielding properties in composite materials<sup>12-14</sup>. Though their microwave-absorbing and heating properties are well-known, practical applications of these phenomena are still emerging. The thermal response of carbon nanotubes to both RF and microwave frequencies has been applied experimentally in the fields of medical technology<sup>6,9</sup> and materials processing<sup>5,11</sup>, but further applications remain to be seen. In this work, we will explore the application of carbon nanoparticles as local heaters embedded in thermosetting adhesive, with the ability to selectively heat the adhesive while keeping its surrounding at a lower temperature.

One quantity that can be used to evaluate the heating response of materials to electromagnetic radiation is the dielectric loss tangent, found by the following equation:

---

\* Part of this section is adapted with permission from “Detection of carbon nanotubes in biological samples through microwave-induced heating” by Irin *et al.*, 2012. *Carbon*, 50, 4441-4449, Copyright [2012].

\* Part of this section is adapted with permission from “Welding of 3D-printed carbon nanotube-polymer composites by locally induced microwave heating” by Sweeney *et al.*, 2017. *Science Advances*, 3, e1700262, Copyright [2017].

\* Part of this section is adapted with permission from “Radio frequency heating of carbon nanotube composite materials” by Sweeney *et al.*, 2018. *ACS Applied Materials and Interfaces*, 10, 27252-27259. Copyright [2018].

$$\tan \delta = \frac{\omega \epsilon'' + \sigma}{\omega \epsilon'}$$

The dielectric loss tangent is defined the ratio between a material's lossy reaction to the electric field portion of an electromagnetic wave to its lossless reaction. Put simply, a higher dielectric loss tangent indicates that a material will dissipate more heat in response to electromagnetic energy. For reference, at a frequency of 2.45 GHz, water has a loss tangent of 0.157. Conventional domestic microwave ovens operate on the principle that the water molecules found in most all foods will react strongly to this frequency of radiation and generate heat; with a loss tangent of 0.157, water provides this heating sufficiently. In **Table 1**, representative values of  $\tan \delta$  for various forms of carbon at 2.45 GHz are presented.

**Table 1** - Loss tangent measurements for various carbon allotropes at 2.45 GHz

Carbon Type	$\tan \delta$
Multi-walled CNTs	0.25-1.14 <sup>15</sup>
Carbon black	0.35-0.83 <sup>15</sup>
Graphene*	0.06-0.09 <sup>16</sup>
Graphite powder	0.43-0.67 <sup>17</sup>

\*data only available at 7.44 GHz

The utility of carbon nanoparticles as microwave-susceptible heaters comes from their uncommonly large dielectric loss tangent. While carbon nanotubes can vary in morphology and chirality, due to the variety in production methods, they seem to be the

carbon allotrope with the most potential for microwave heating. A quick review of the literature shows more results using carbon nanotubes than any other carbon allotrope. However, other forms of carbon, including micro-scale graphite powder and nano-scale carbon black, show potential for similar, but reduced, heating responses to microwaves.

A more tangible method of characterizing EM response is to empirically observe a materials' heating response. For the paper Irin *et al.* (2012), our group categorized the heating responses for various pure forms of carbon particles<sup>10</sup>. At a microwave frequency of 2.45 GHz and power of 30 W, 1 mg of each carbon sample was irradiated for 1 second, making note of initial and final temperatures via a thermocouple. The results can be seen in **Table 2** (adapted from Irin *et al.*, 2012<sup>10</sup>).

**Table 2** - Heating response of 1 mg samples of carbon to 1 second of microwave radiation (2.45 GHz, 30 W) (adapted from Irin *et al.*, 2012)

Sample	T <sub>initial</sub> (°C)	T <sub>final</sub> (°C)
Multi-walled CNTs	25	714
Carbon black	25	348
Graphene powder	25	83
Graphite flakes	25	156

As expected from the dielectric loss tangent analysis, carbon nanotubes showed the most drastic heating response. Carbon black still showed an impressive heating response, with a  $\Delta T$  of 323°C after just one second of microwave irradiation.

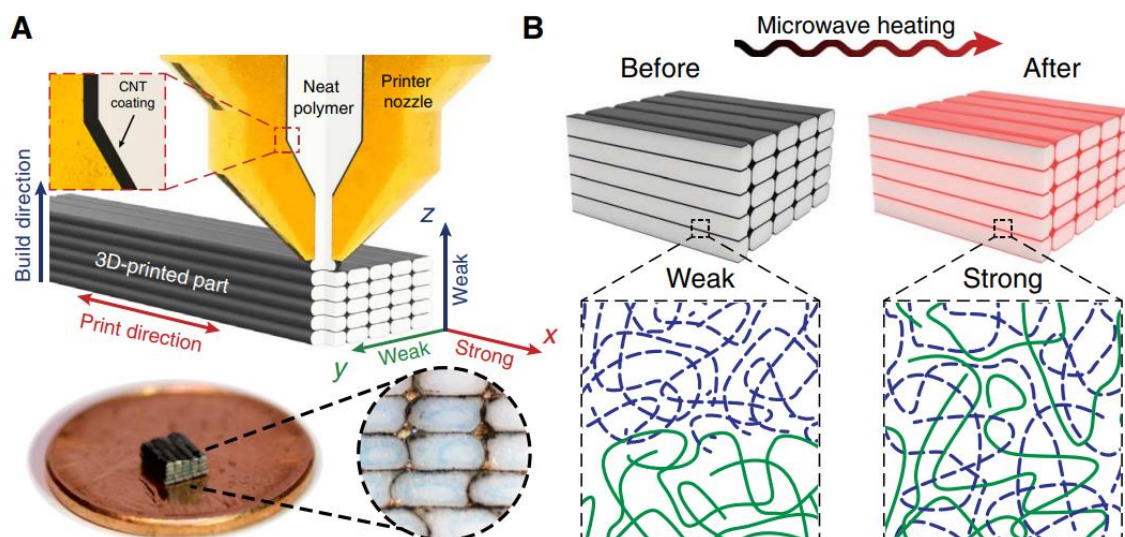


**Figure 1** - A) 3D-printed parts using carbon nanotube ink-coated printer filament and B) the effect of microwave heating at the interfaces between print layers (reproduced from Sweeney *et al.*, 2017)

Some research groups have used carbon nanotubes as microwave susceptors for the purpose of rapid, localized heating during material processing<sup>7,18,19</sup>. In the paper “Welding of 3D-printed carbon nanotube–polymer composites by locally induced microwave heating” (Sweeney *et al.*, 2017), our group sought to solve one of the major issues with 3D printing with thermoplastic polymers: weak interfacial bonds leading to poor tensile strength in directions orthogonal to the print direction (see **Figure 1**)<sup>18</sup>. A composite ink containing carbon nanotubes was applied to the surface of 3D printing filament, and a fully printed structure made using this filament was exposed to microwaves at 2.45 GHz. The carbon nanotube ink heated in response and melted the interfaces between print layers in the structure, effectively welding them together. Fracture strengths improved by up to 275% by applying the CNT ink and using this microwave welding

technique. The selective nature of the heating achieved through microwave excitation of nanotubes is the most integral part of this paper. The technique of heating a 3D printed part to weld together its layers had been attempted before; however, applying external heating to post-printing structures often resulted in global morphology deformation. Using the CNT ink, our group was able to selectively target only the interfaces between print layers with heating, welding them together without observing overall structural deformation. This selective heating is what pushed our group to investigate further applications of this technology.

Recently, our group has demonstrated that lower frequencies can be used to accomplish this same heating response. In our paper “Radio Frequency Heating of Carbon Nanotube Composite Materials” (Sweeney *et al.*, 2018), we characterized the heating response of a nanotube-loaded composite polymer in the frequency range of 1-200 MHz

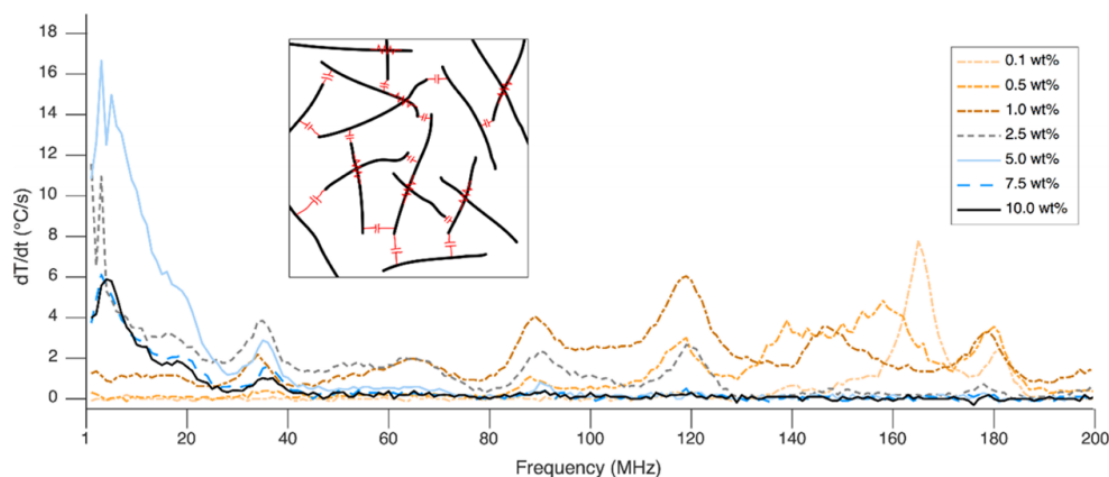


**Figure 2** - Heating response of MWCNT/PLA composite films of varying wt% MWCNTs to various radio frequencies (reproduced from Sweeney *et al.*, 2018)



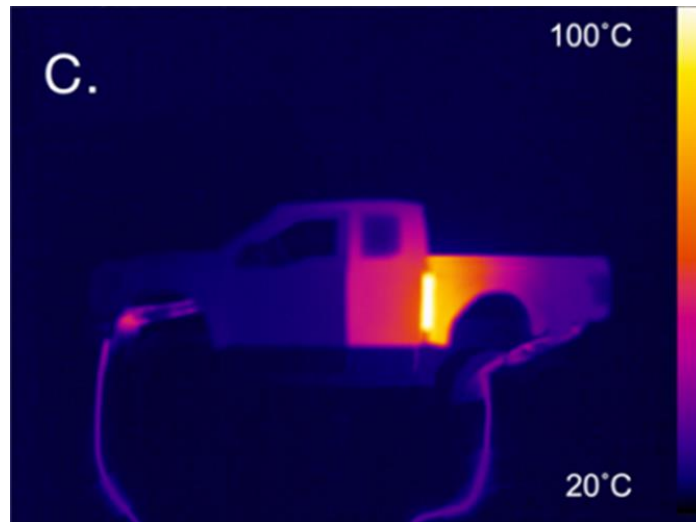


**Figure 3** - Heating of a carbon nanotube/epoxy composite using RF energy (adapted from Sweeney *et al.*, 2018)

(**Figure 2**), and utilized RF heating at frequencies of 50 and 100 MHz to rapidly heat a one-part thermoset epoxy (**Figure 3**)<sup>19</sup>. This was a relatively new discovery, as most all literature using carbon nanoparticles as heating elements had focused on using microwaves. RF heating is better than microwave heating for a few key reasons. First, RF waves are capable of greater penetration depths, owing to their larger wavelengths. Second, RF waves can impart heating more uniformly; this is because RF is transmitted primarily by applicators, which can be specially and carefully designed, while microwaves are primarily applied through a waveguide, a method of application which induces various random elements. Third, RF is capable of better selectivity; in the frequency range of microwaves, the loss tangents of materials tend to be more similar, whereas at radio frequencies, a great many more materials have comparatively low loss tangents, making them “invisible” to RF heating, and allowing a select few materials to be used purposefully

as RF susceptors. Lastly, radio frequencies are safer to humans. Microwaves can cause severe burns, by heating human tissue in the same way they heat up food: by exciting the many water molecules in our body. For this reason, microwaves have to be contained in waveguides or Faraday cages to prevent injury to users. Radio frequency waves are much safer for humans, as they do not cause painful thermal burns, and according to the American Cancer Society, it is unlikely that they cause cancer or promote tumor growth<sup>20</sup>. If the same heating response from carbon nanoparticles can be obtained using radio frequencies, there is little reason to continue using microwaves.

The primary method of applying RF energy to the desired sample we used in Sweeney *et al.* (2018) is direct contact. In this method, the highly conductive substrates to be bonded together (in our case, two metal parts) serve as the electrodes of a capacitor, between which the RF field is generated. The RF signal is transmitted to the sample by means of a coaxial cable, with the inner conductor of the cable attached to the “hot” electrode, and the outer conductor attached to the “ground.” This method proved to be a highly efficient way of applying RF energy to the target adhesive. However, in this work, the main focus of our research is bonding together plastic coupons; such coupons are quite different from the substrates in the prior work in one major regard: the plastic is many orders of magnitude less conductive than metal. For example, the conductivity of polypropylene<sup>21</sup> is approximately  $1 \times 10^{-15}$  S/m, while the conductivity of aluminum<sup>22</sup> is  $3.7 \times 10^7$  S/m. Polymers are not sufficiently good conductors for transmitting RF energy; therefore, in this work, we utilized a “non-contact” method of RF application, involving

the fringing field of a coplanar plate capacitor. More information about this applicator can be found in section 3.2.1.

## **2.2. The need for localized heating in adhesive bonding**

In general, most adhesives show better performance when cured at higher temperatures. There are many commercial adhesives that are marketed as being able to cure at room temperature, and to be sure, they can achieve great strengths just from being at room temperature for the specified time; however, in actuality, most of these adhesives would attain an even higher degree of cure if they were cured at a higher temperature<sup>23</sup>. Recommended temperatures for curing adhesives can range from  $\sim 150^{\circ}\text{C}$ , which is relatively common, to  $250\text{-}300^{\circ}\text{C}$  for specialty applications. Heating adhesives to these temperatures can often pose several technical challenges in industrial applications, such as selecting the correct heating method, or accounting for the time added to the process. One potential issue is the susceptibility of the bonding substrates to these high temperatures. In the case of bonding together plastic components, there are two temperatures to take note of: glass transition temperature ( $T_g$ ) and melting temperature ( $T_m$ ). The glass transition temperature marks the temperature at which a polymer transitions from a hard “glassy” state into a softer, more rubbery state. Some plastics are intended to be used below their  $T_g$ , in the brittle region, while others are intended to be used above the  $T_g$ . Heating a plastic above its  $T_g$  causes it to soften and deform; such deformation is frequently undesirable, which makes  $T_g$  an upper limit that must be avoided. Another deformation effect is also observed at the melting temperature ( $T_m$ ), the

temperature at which a solid material loses any long-range order it has and transitions into a liquid state. Any plastic heated above its  $T_m$  will experience structural deformation by melting, or worse, structural degradation. To avoid deformation of plastic components, certain adhesives which cure at temperatures near these transition temperatures cannot be used. Some common structural plastics that might be affected by the high temperatures needed to cure some adhesives include poly(vinyl acetate) ( $T_g = 34^\circ\text{C}$ ), poly(vinyl fluoride) ( $T_g = 53^\circ\text{C}$ ), PVC ( $T_g = 83^\circ\text{C}$ ), Polystyrene ( $T_g = 100^\circ\text{C}$ ), PMMA ( $T_g = 105^\circ\text{C}$ ,  $T_m = 144^\circ\text{C}$ ), Teflon ( $T_g = 119^\circ\text{C}$ ), polyethylene ( $T_m = 141^\circ\text{C}$ ), and polypropylene ( $T_m = 173^\circ\text{C}$ ). It is important to note that these temperatures are for the plastic's basic formulation, and that the addition of additives may increase or decrease these values slightly.

Another challenge that might be faced is the case of bonding dissimilar metals using heat-curing adhesive. Every metal has an intrinsic property called the coefficient of thermal expansion, given by the equation:

$$\alpha_v = \frac{1}{V} \left( \frac{\partial V}{\partial T} \right)_P$$

This property is a measure of how much a metal will expand when heated, and it varies from metal to metal. This means that when heated over the same  $\Delta T$ , two metals will expand different amounts. This can cause stress between two metal parts that are meant to be bonded. For example, if a part consisting of two dissimilar metals is intended for use at room temperature ( $23^\circ\text{C}$ ), and the adhesive with which they are to be bonded has a curing temperature of  $160^\circ\text{C}$ , one metal will want to expand away from the other as the system heats up. The adhesive then cures with the metals in this expanded state, and as

the system cools, the more expanded metal imposes a stress upon the adhesive as it tries to return to its original shape. This can result in an overall weakening of the adhesive joint. If the metals could be kept at a lower temperature during the curing of the adhesive, there would be less deflection between the two parts and less residual stress in the joint upon returning to room temperature.

The targeted heating possible using carbon nanoparticles and RF could be used to expand the range of adhesives appropriate for bonding together systems of plastics or metals. By selectively heating the nanoparticle composite adhesive, the overall heat of the substrates can be kept lower. Using a conventional heating method, like an oven or IR lamp, the heat comes from an external source, and must penetrate the substrate before heating the adhesive. This means that the substrates will always be at least as hot as the adhesive, and will often be hotter. With RF heating, the heat comes from within the adhesive, generated by the carbon nanoparticles in response to the RF field. It is then possible for the adhesive to be at curing temperature while the substrates are kept at a lower temperature.

### **2.3. New approach: Application of carbon nanoparticles as local heaters**

Here we demonstrate the viability of using carbon nanomaterials, specifically carbon black, to induce localized heating in heat-curing adhesives. Radio-frequency electromagnetic waves can be generated in a sample of adhesive via an RF applicator; in this work, we use a coplanar strip capacitor and utilize the fringing electric field generated in the space above and between the electrodes. These RF waves are absorbed by the carbon

black embedded in the adhesive matrix, causing a rapid and localized heating response. In some samples, the adhesive reached the target temperature of 85°C within 40 seconds, and maintained a temperature at least 28°C hotter than the hotter of the two substrates. The samples were cured for 2 minutes at temperature, and lap shear testing was conducted on the samples 35 minutes later. Shear strengths of all samples were found to be reliably above the recommended handling strength of 1 MPa (145 psi). The successful application of this RF heating technology could widen the range of potentially appropriate heat-curing adhesives that can be used on thermally sensitive substrates, such as plastics and metals, and could greatly improve manufacturing efficiency by reducing time needed to cure a part on an assembly line.

### 3. EXPERIMENTAL METHODS AND RESULTS

#### 3.1. Materials and Procedures

##### 3.1.1. Materials

The plastic substrates and adhesive used in this experiment were supplied by Dow Chemical Company, as were all the tools needed to handle and process these materials. The butane torch was purchased from Cole-Parmer®. The RF signal generator was purchased from RIGOL Technologies. The RF signal amplifier was purchased from Prâna. The lap shear testing instrument was purchased from MTS Systems.

##### 3.1.2. Procedures

###### 3.1.2.1. *Sample preparation*

The lap joint samples prepared in this experiment are compliant with ASTM standard D3163-01. The two plastics used in our experiments are both forms of polypropylene. The long glass fiber polypropylene (LGFPP) coupon represents the “base” part, to which the outer layer is being adhered. The thermoplastic olefin (TPO) coupon represents the outer surface, through which the RF energy is applied to irradiate the adhesive. The large sheets (3 mm in thickness) of LGFPP and TPO supplied by Dow were cut into coupons with a width of 1 inch and a length of ~4 inches. The last inch of each coupon was flame treated with the butane torch at a medium-low setting, sweeping the flame back and forth across the surface for ~10 seconds per coupon, so as to functionalize the bonding surface without deforming the coupon. On the flame-treated surface, a

priming solvent (provided by Dow) was applied with a small cotton-swab type brush, to aid this particular adhesive in bonding to the plastic coupons. Plastic spacers made of polyetherimide of thickness 1 mm were placed on the bounds of the bonding area, ½ inch apart, to make sure the bond thickness would be a uniform 1 mm.

The adhesive used in these experiments was a two-part, polyurethane-based adhesive, called Dow BETASEAL™ X2500 PRIME, parts A and B. This adhesive formulation contains 10-15 wt% carbon black when mixed; this is the source of the carbon nanoparticles we targeted for RF heating. The two parts were combined using a dynamic mixing tool. Once extruded, a small amount of adhesive was transferred to the primed TPO surface and spread evenly 1 mm thick. The LGFPP coupon was pressed on top of the bond area, and the excess adhesive was wiped away. A piece of kapton tape was used to hold the two coupons together while the adhesive was still uncured.

For some adhesives, proper application requires the use of a surface primer. Primers are generally used to ensure effective link-up between the adhesive and the surface to which it is applied. Without a primer, the adhesive can fail at the adhesive-substrate interface (adhesive failure) as opposed to failing down the middle of its own volume (cohesive failure). Getting cohesive failure is the best way to observe the true strength of adhesive joints, so proper primer use is critical when making samples.

#### ***3.1.2.2. RF field application and thermal data acquisition***

A RIGOL DSG815 model signal generator was used to generate the RF signals used. The signal was amplified (up to powers of 100 W) by a PRANA GN500 model broadband power amplifier. This signal was delivered an applicator of our own design by



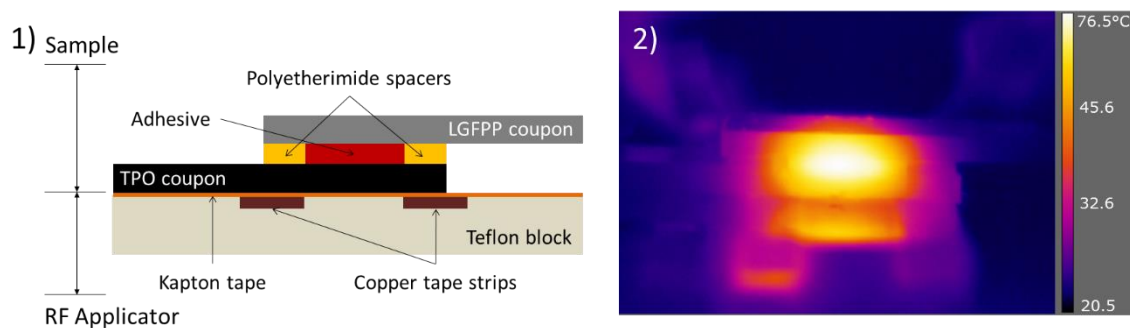


**Figure 4** - 1) Side-view schematic detailing the experimental setup of the sample and the RF applicator, and 2) Side-view thermal image of a sample being subjected to RF energy at 116 MHz

50 $\Omega$  coaxial cables. The applicator consists of two strips of ¼-inch wide copper tape, laid parallel with ½ inch of space between them, running ~3.5 inches along the top of a small block of Teflon. One copper strip is connected to the inner conductor of the coaxial cable, and the other copper strip is connected to the outer conductor. Upon the application of RF energy, this setup generates a strong electric field in the gap between the two copper strips, along with a fringing electric field in the volumes directly above and below this gap (see **Figure 5**). We utilize this fringing electric field to apply the RF energy to the carbon black nanoparticles in the adhesive.

To collect temperature data for the adhesive and the two substrates during the RF heating process, we utilized a FLIR® A655sc model infrared camera, along with FLIR® ResearchIR Recording and Analysis software. Thermal data was acquired by viewing the sample from the side with the FLIR camera as it sat atop the applicator. This setup can be seen in **Figure 4**. The maximum temperature of the adhesive section was monitored to ensure there were no hotspots above 100°C (the degradation temperature of the adhesive).

For the TPO and LGFPP substrates, the mean temperature of the area directly above or below the adhesive was taken.

#### ***3.1.2.3. Lap shear testing***

The goal of this work was to use RF heating to quickly cure thermosetting adhesive to a sufficiently high strength so that the part could be handled and processed, referred to as “green strength,” while keeping the temperature of the heat-susceptible substrates below their processing temperatures. This goal was inspired by an industrial manufacturing-focused motivation: to use the quick heating of RF to spot-cure selected sections of a large adhesive area to impart handling strength on the whole part. This would allow large parts bonded with adhesive to be moved down an assembly line without needing to wait for the adhesive to achieve full degree of cure.

In order to test for shear strength, we bonded two plastic coupons into a simple lap joint. The cured samples were lap shear tested using an MTS Insight® Electromechanical Testing System. Pneumatic clamps were used, with a gripping pressure of 70 psi. Two 1-inch by 1-inch squares of TPO and polyetherimide plastic were cut to be affixed to the ends of the finished samples, to ensure the samples had proper vertical alignment when clamped. Using the MTS Testworks® software, a simple tensile test was performed at room temperature, with a crosshead speed of 2 in/min. Upon detection of failure, the coupon was removed, and pulled completely apart to expose the fracture surface for analysis. The shear strength in psi of the samples was determined by dividing the maximum load sustained by the sample in pounds by the bond area in square inches.

#### ***3.1.2.4. SEM surface characterization and optical microscopy***

The fracture specimens were mounted on SEM stubs and sputtered with 10 nm thick Iridium coating. The Iridium coating mitigates charging due to the electron beam, thereby providing better images. LYRA3 TESCAN FE-SEM was used to image the fracture surfaces using 10 kV electron beam. SEM analysis was carried out to investigate the fracture surface morphology and determine particular toughening mechanisms initiated by the carbon black particles in the nanocomposite adhesive.

### **3.2. Results**

#### **3.2.1. Design of the RF applicator**

An RF applicator is a device that “applies RF/microwave energy into a material volume at a level sufficient to create either a permanent or temporary change in a material

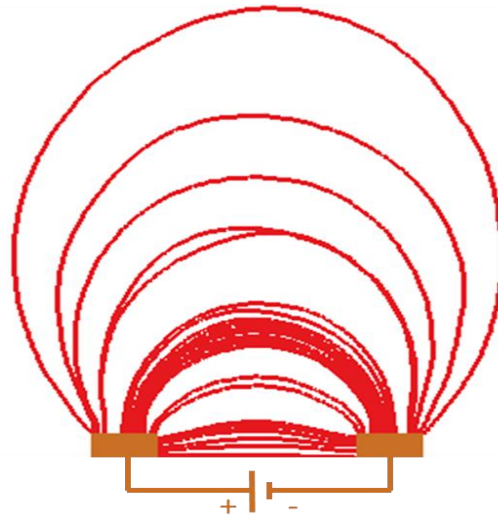


**Figure 5** – COMSOL model of the fringing electric field in the volume above a coplanar plate capacitor

parameter or property.”<sup>24</sup> In our case, we use an RF applicator to excite carbon nanoparticles, generating heat and raising the temperature in our adhesive. The design of the applicator had to be carefully considered in order to efficiently heat the target volume with the RF field passing through the substrates. The base design was a coplanar plate capacitor (see **Figure 5**). For this type of capacitor, the fringing electric field is stronger and acts over a larger volume than in a parallel plate capacitor, though it decays exponentially with height. The capacitor is made from two strips of copper tape laid down on a block of Teflon. One copper strip is connected to the inner conductor of the coaxial cable, and the other copper strip is connected to the outer conductor. The fringing field is most powerful in the volume directly above and between the copper strips.

Our original applicator design had the copper strips placed 3 mm apart. After curing samples and characterizing their lap shear response, it was determined that the applicator was not providing RF heating to a large enough area of adhesive. The desired volume of adhesive was 1 mm thick, with an area of 1-inch by ½-inch. After the joint failed, we observed that curing had only occurred in a thin strip ~8 mm wide, centered on the part of the adhesive that sat directly above the applicator. Due to the precise nature of RF heating with nanoparticles, the only part of the adhesive that heated enough to initiate curing was directly above the space in between the capacitor’s electrodes; the rest of the adhesive saw heating only by conduction from the RF-excited region. In order to cure a larger area evenly, we would need a different design of applicator

The first redesign was inspired by an applicator used in our prior work “Radio Frequency Heating of Carbon Nanotube Composite Materials,” by Sweeney *et al.*

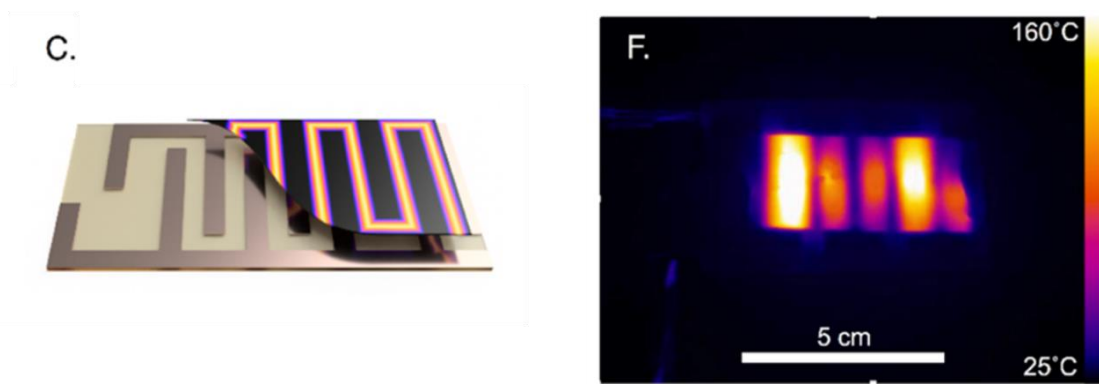


**Figure 6** - Excerpt from Figure 2 of Sweeney *et al.* (2018), showing (C) the geometry and expected heating profile of the interdigitated capacitor, and (F) a FLIR thermal image of a composite MWCNT/PLA thin film being heated by this capacitor

(2018)<sup>19</sup>. “Interdigitated fingers” of copper tape formed the two electrodes of the capacitor, and the fringing field was developed in between the fingers, resulting in a serpentine pattern of heating in samples (see **Figure 6**). If the serpentine pattern could be made sufficiently thin enough, it would generate approximate even heating over a whole rectangle of adhesive. To this end, a new interdigitated capacitor was created with half-width strips of copper tape and decreased spacing between the fingers. This new applicator’s heating capacity was characterized with a test sample of 1 mm thick adhesive spread over a 3 mm thick TPO coupon, left open-face to view the entire adhesive area from the top. No heating from the sample was observed, even at maximum power level. Decreasing the cross sectional area of the copper strips decreased the overall capacitance, but also (unexpectedly) decreased the heating level. Mehdizadeh (2010) refers to a variable called Effective Field Volume (EFV), which is defined as the region in or around an applicator where the RF field produces measureable results<sup>24</sup>. With the thinner fingers of the new interdigitated capacitor design, the EFV was limited to less than 3 mm above

the capacitor; this was not large enough to penetrate the outer TPO layer and impart enough energy into the adhesive to produce heat. For this type of applicator to work, thicker electrode strips are required; however, since the electrodes cause “dead zones” in the heating pattern, this would result in a more pronounced serpentine heating pattern. If an even rectangle of heating is desired, using an applicator of this design would be too problematic.

The original simple coplanar plate capacitor was redesigned with a 13 mm spacing between the plates, enough to evenly heat a strip of adhesive ½-inch wide (see **Figure 4**). Samples were made with a bond area of 1-inch by ½-inch and an adhesive thickness of 1 mm. From the test sample in **Figure 7**, a much wider area of heating was observed

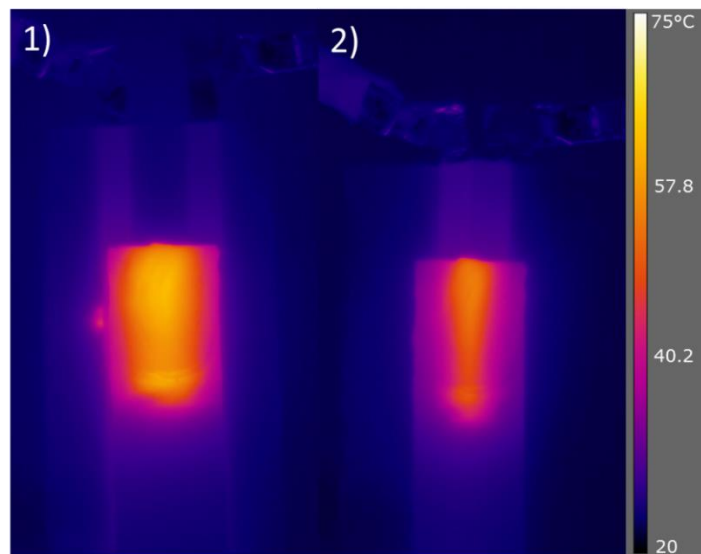


**Figure 7** - Top view of the thermal response of ~2 mm of adhesive on top of a TPO coupon, after 5 minutes of RF exposure (32 W, 116 MHz) using applicators with 1) 13 mm spacing (½ inch), and 2) 3 mm spacing

compared to the initial design. At an initial power of 100 W and a frequency of 116 MHz, the entire adhesive area could be heated to the target temperature of 85°C within ~40 seconds. This applicator design was then used for all experiments involving lap shear strength tests. However, scalability for this design does pose certain challenges. First, theoretically, given a high enough initial power, any target temperature could be reached in 2-3 seconds. The power input is limited by the material between the capacitor plates, however, as at high enough voltages, dielectric breakdown can occur, causing arcing which could potentially damage the applicator. Second, as desired bonding area increases, one could modify the dimensions of the capacitor. The capacitance of this coplanar model is given by the following equation:

$$C = \frac{\epsilon_r l \ln \left( -\frac{2}{\sqrt[4]{1 - \frac{s^2}{(s+2w)^2}} - 1} \left( \sqrt[4]{1 - \frac{s^2}{(s+2w)^2}} + 1 \right) \right)}{377\pi v_0} \text{ for } 0 < \frac{s}{s+2w} \leq \frac{1}{\sqrt{2}}$$

$$C = \frac{\epsilon_r l}{120 v_0 \ln \left( \left( -\frac{2}{\sqrt{\frac{s}{s+2w}} - 1} \left( \sqrt{\frac{s}{s+2w}} + 1 \right) \right) \right)} \text{ for } \frac{1}{\sqrt{2}} < \frac{s}{s+2w} \leq 1$$

where  $w$  is the width of the plates,  $s$  is the spacing between them,  $\epsilon_r$  is the relative permittivity of the insulator between the plates,  $l$  is the length of the plates, and  $v_0$  is the speed of light in a vacuum. As width increases or separation decreases, capacitance increases, increasing the strength of the generated electric field and the size of the EFV.

For systems that use RF applicators for heating, there will be some frequency at which maximum heating is achieved, called the resonant frequency<sup>24</sup>. The resonant frequency of a system is dependent on that system's impedance, a complex property that takes into account the capacitive and inductive elements of both the RF applicator and the material load (the target of the RF heating). Maximum heating is achieved when the impedance of the RF source is matched with the impedance of its system. Because the impedance of a system is a function of frequency, by changing the frequency at the RF source, one can "tune" the system for maximum heating. For our coplanar plate applicator, from past experience, we knew the optimal frequency would lie between 50-150 MHz. By analyzing instantaneous heating rate at different frequencies, a "resonant frequency" for any combination of applicator and material load can be obtained. We manually tuned our system, consisting of our designed applicator and the samples we intended to cure, by incrementing frequency and observing which frequency resulted in the largest instantaneous heating; we determined this resonant frequency to be 114 MHz.

### **3.2.2. Thermal data: Adhesive and substrates**

**Figure 8** shows a comparison of heating using an IR bonding device to RF heating. Using RF energy at a frequency of 114 MHz and with an initial power of 100 W, we were able to heat the adhesive in the sample to a temperature of 85°C in ~ 40 seconds. This is much more potent heating than is observed with the IR bonder, with RF able to heat the adhesive 16 degrees higher than the IR bonder in less than one third the time. During the RF heating process, power was reduced steadily as the experiment went on, to maintain



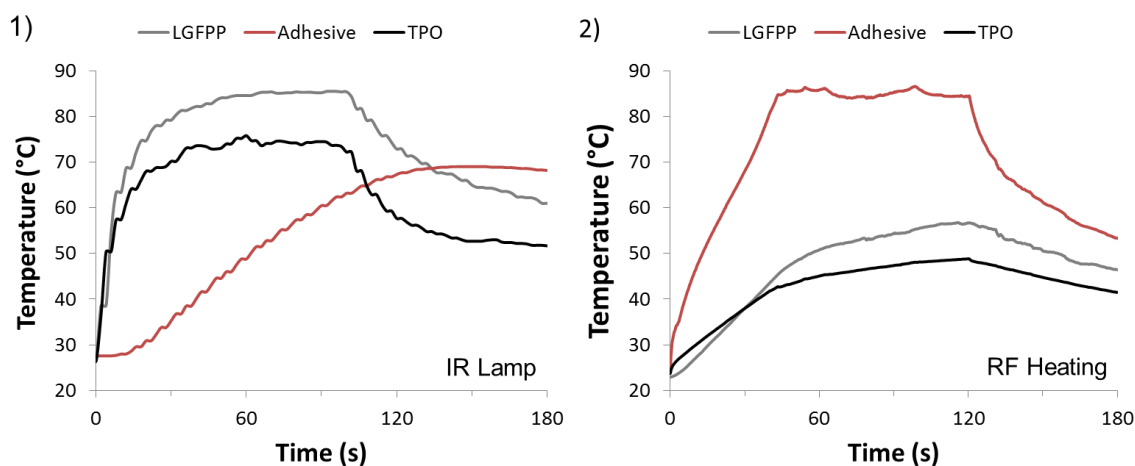


**Figure 8** - Temperature profiles of samples during heating using 1) an IR lamp (data captured using thermocouples) and 2) RF heating (data captured using FLIR camera)

the adhesive at the target temperature. Due to the exothermic polymerization reaction and the buildup of heat in the system, the temperature of the adhesive naturally continues to increase, requiring less RF energy input to remain at 85°C. For most samples, at the end of the 2 minutes of RF exposure, the RF source was supplying only 20 W of RF energy.

At the end of the 2 minutes of RF heating, the LGFPP reaches an average temperature of 58.2°C, and the TPO reaches an average temperature of 52.8°C. These are well below the maximum temperatures reached by the substrates in the IR bonder, where LGFPP would reach 85.5°C and TPO would reach 75.8°C. This difference in the temperatures of the substrate is due to the targeted heating provided by the carbon black nanoparticles. As long as the substrates contain no RF-active nano-fillers, they will not be heated by the RF field, receiving heat only from the adhesive by thermal conduction. By contrast, in the IR bonder, the IR lamps directly heat the outer substrates, and the heat must penetrate into the interior of the joint to heat the adhesive.

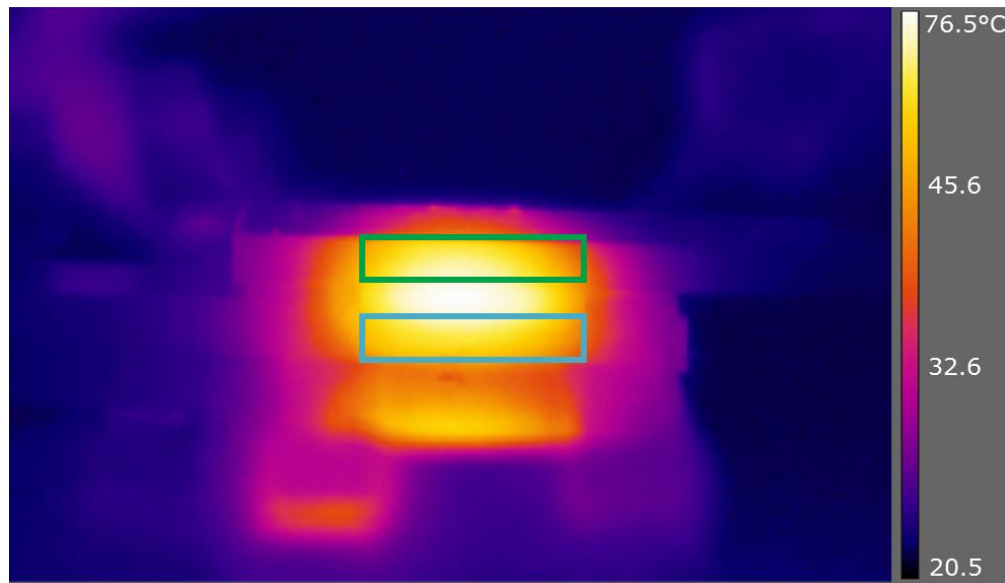


**Figure 9** - The areas over which mean temperature was calculated are shown for LGFPP (green) and TPO (blue)

**Figure 9** shows an example FLIR image used in thermal data acquisition. The mean temperatures for TPO and LGFPP were calculated over the areas shown. We chose these areas to get the most accurate approximation for the substrate temperature possible; the hottest part of the substrate would be the area directly adjacent to the curing adhesive. The maximum temperature of the adhesive was measured over the entire lap joint. Maximum temperature was chosen over mean temperature for the adhesive to avoid thermal degradation of the adhesive anywhere due to hotspots. All of these temperature measurements were taken from the side. A limitation of this side view is that we can't observe exact temperature over the entire volume of the substrates or the adhesive. Due to limitations on heat transfer, the hottest point of the adhesive would be directly in the middle. In an attempt to further avoid thermal degradation of the adhesive (initiated at 100°C), we targeted a maximum temperature of 85°C in the side view.

### 3.2.3. Mechanical data: Lap shear testing and shear strength

In order to assess the green strength of the adhesive joints, lap shear tests were carried out shortly after curing. After 2 minutes of RF exposure, the samples were transported to the Materials and Testing Lab in the department of aerospace engineering. A simple tensile test was carried out to determine the maximum sustainable load for each sample. This value was divided by the bond area to determine shear strength. As a general rule of thumb for determining green strength in adhesives, 1 MPa (~145 psi) is considered “light handling strength,” so this was the criteria used for determining success in samples. Ideally, green strength would be tested as soon as possible after the adhesive joint was cured; however, our tensile testing equipment was in a different building than our RF setup. As a result, lap shear testing could be completed no sooner than 35 minutes after curing the samples. This is notable in that it gives us higher values of green strength than we would see 35 seconds after cure, but likely not to any appreciable degree. According to an old rule of thumb for reaction kinetics, reaction rate doubles with every 10°C increase. Our adhesive curing reaction took place at 85°C, while the temperature of the adhesive during transport to the lap shear machine was ~25°C, so crosslinks in the adhesive were forming approximately 64x slower after heating stopped. Thus, the added contribution to shear strength of the time of transportation to the Aerospace Materials and Testing Lab only amounts to ~30 extra seconds of RF curing.

The results of the lap shear tests can be seen in **Figure 10**. We were able to get fairly repeatable shear strength results between multiple different samples: the average shear strength was 472.8 psi, with a standard deviation of 58.4 psi. These results are

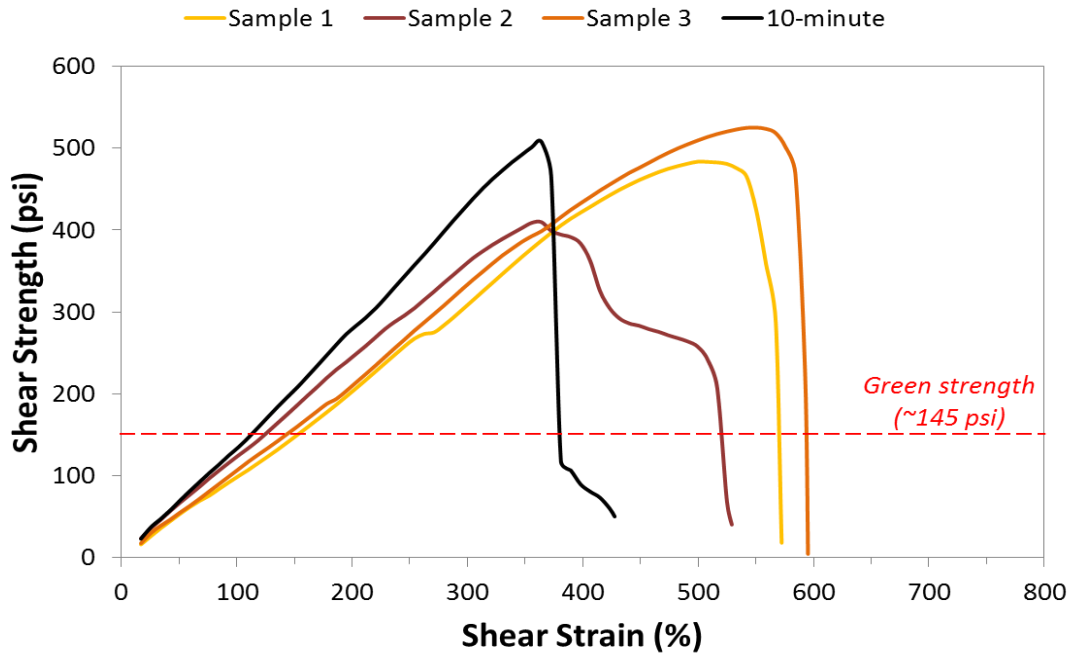


**Figure 10** - Stress-strain curves for samples cured at 85°C for 2 minutes, with a sample cured for at 85°C for 10 minutes for comparison

incredible for adhesive cured for only 2 minutes at temperature, showing strength values roughly 300% that of the green strength.

It is interesting to note the shear moduli of the samples, which is an indicator of degree of cure in an adhesive. The shear modulus of a material is equal to shear stress divided by shear strain:

$$G = \frac{\tau}{\gamma} = \frac{\frac{F}{A}}{\frac{\Delta x}{l}}$$

where  $F$  is applied load,  $A$  is shear area (bond area),  $l$  is the thickness of the material (the adhesive), and  $\Delta x$  is the transverse displacement. This value can be determined from the

slope of a stress-strain curve, and is a measure of how much a material deforms under shear stresses. In **Figure 10**, the stress-strain curves for selected samples are compared to that of a sample that was RF-cured at a target temperature of 85°C for 10 minutes. The adhesive in this 10-minute sample would have been cured to a high degree of polymerization, meaning the sample would have the shear modulus near that of fully-cured adhesive. The shear moduli of the samples cured for 2 minutes seem to vary a bit between tests; however, they are all very similar to that of the 10-minute sample, showing similar stiffness and resistance to strain under the same load. From this, it can be inferred that even 2 minutes at temperature is enough to highly cross-link this adhesive. To save more time and still achieve a strength greater than the green strength, the RF field could be applied for an even shorter duration.

In **Figure 11**, we show a comparison of lap shear tests conducted on samples cured using an IR Bonder (data supplied by Dow Chemical) and cured using RF heating. The procedure for the IR bonder is to heat the sample for 90 seconds using a bulb temperature of 80°C, leave the sample in the bonder an additional 90 seconds while the substrates cool down, and then let the sample stand a specified length of time before tensile testing. The procedure for RF heating is to heat the sample to 85°C and hold it at that temperature for a specified length of time, immediately turn off the RF source, then let the sample stand for 30 minutes while it was transported to the tensile testing machines. The dimensions of the IR bonder samples are 0.25" x 0.25" x 1", with the tensile test working in the 1" direction. The dimensions of the RF samples are 0.04" x 1" x 0.5", with the tensile test working in the 0.5" direction.

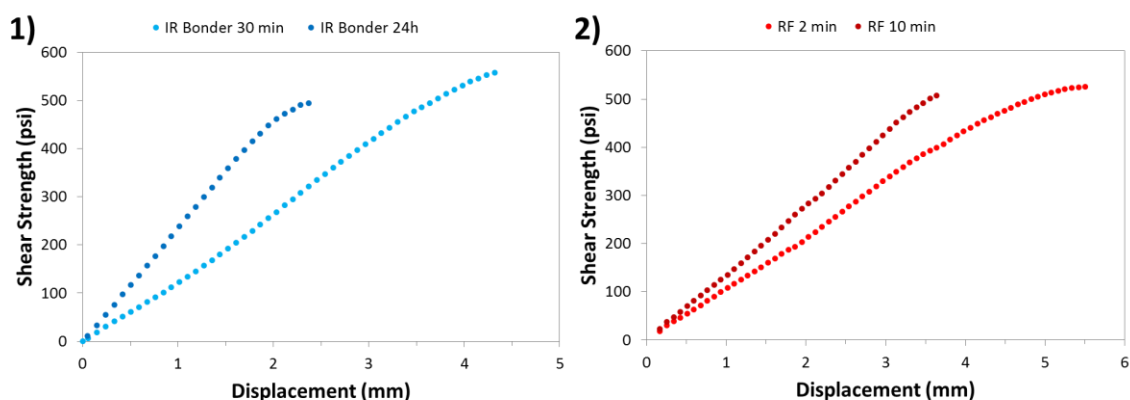


**Figure 11** - Stress vs. displacement curves for lap joint samples using 1) the IR bonder (heat for 3 minutes, let stand for specified time) and 2) RF heating (heat for specified time, let stand for 30 minutes)

Because they were both allowed to stand for 30 minutes, the RF samples are most comparable to the “IR Bonder 30 min” sample, henceforth called the “IR sample,” in terms of strength and shear modulus; the “IR Bonder 24h” sample, henceforth called the “fully-cured sample,” was included in the graph for the sake of comparison to fully-cured adhesive. Both of the RF samples failed around 500 psi, with the 2-minute sample experiencing more strain up to this point. The IR sample failed around 550 psi, with a strain similar to the 10-minute RF sample. There is little difference in achievable strength between the two bonding methods. Though the RF samples achieve shear strengths comparable with the fully-cured sample, they have lower shear moduli. This means that this adhesive can attain full strength without being cross-linked to completion. From this data, we can see there is no added strength benefit gained by using RF curing, but neither are there any negative side effects that reduce adhesive strength.

### 3.2.4. SEM imaging: Toughening mechanism & adhesive weakening near carbon black

We conducted SEM imaging on the fracture surface of the adhesive post shear testing to further characterize the method by which our nanocomposite adhesive cures and to gain insight into the effects of carbon black on the adhesive matrix. Nanoparticles provide a toughening mechanism when added into a material matrix, by means of crack deflection. Cracks form when a material is under stress, as this added energy provides the means with which to break the inter-molecular bonds holding the material together. When the front of the crack reaches a nanoparticle, whose covalent bonds are orders of magnitude stronger than the inter-molecular forces of the matrix, the nanoparticle resists breaking, and the crack propagates in the matrix around the nanoparticle, as seen in **Figure 12-1**. **Figure 12-2** shows how dispersions of nanoparticles provide extra toughness, by increasing the total length of propagation of the crack, thereby increasing the total energy required to break the material. This is the mechanism we expect to see in our adhesive.

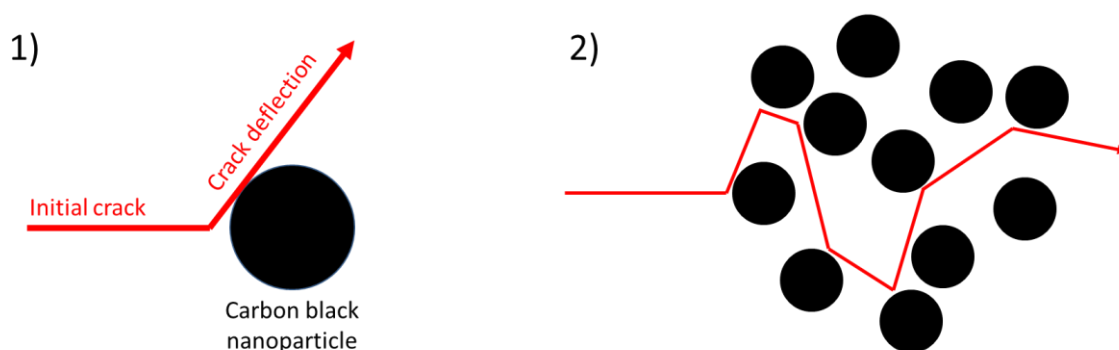


**Figure 12** - Diagrams showing 1) how carbon black nanoparticles deflect cracks into the surrounding matrix, and 2) how dispersions of nanoparticles provide extra toughness by lengthening the path of the crack, increasing the total energy required to propagate it

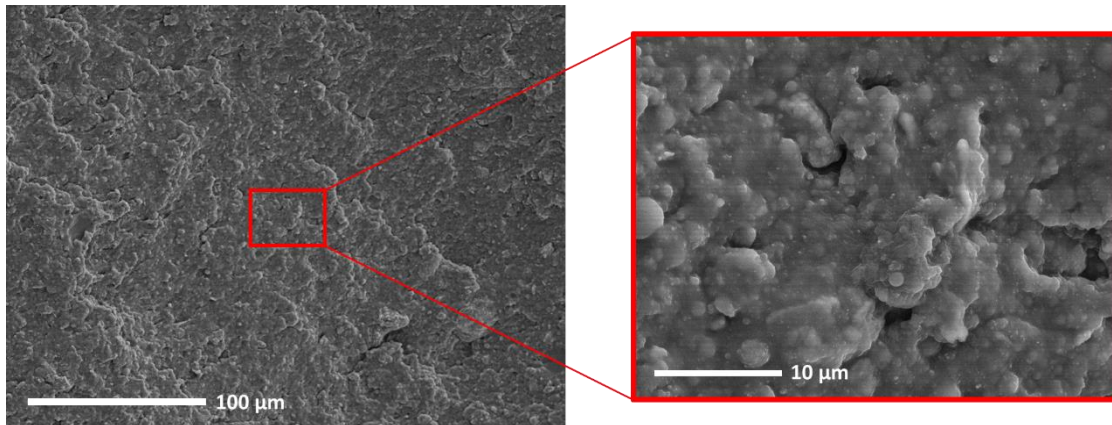


**Figure 13** - SEM images of adhesive fracture surface post shear testing, showing layered failure planes (left) and the semi-rough surface (right)

In **Figure 13**, the shear fracture surface of the adhesive from one of the test samples is shown. This fracture surface was taken in the middle of the adhesive, in a plane of cohesive failure. Cohesive failure is the desired failure mode, as it means the joint fails entirely in the adhesive volume; this is in contrast to adhesive failure, where the link-up between the adhesive and the surface of the substrate is not good, and the fracture plane is partially or completely at the adhesive-substrate interface. From the image on the left, the fracture surface looks rough, with distinct vertical fracture lines delineating different layers of the adhesive. In the image on the right, we get an even closer look at the surface. We do not see carbon black aggregates, indicating good-quality dispersion in the initial uncured matrix. We can also see that the surface roughness exists on the nano scale ( $\sim 100$  nm), where these surface irregularities can be directly attributed to carbon black. In these images, it is apparent that carbon black has a distinct effect on the roughness of the fracture surface, and the overall toughness of the adhesive.



### 3.2.5. Direct contact heating on carbon fiber

As a continuation of the work done by our group in “Radio Frequency Heating of Carbon Nanotube Composite Materials,” by Sweeney *et al.* (2018)<sup>19</sup>, we also investigated using the method of direct contact to apply RF heating to a carbon black-loaded adhesive through carbon fiber-epoxy composite substrates. In the paper, the method of direct contact RF heating required that the substrates to be bonded together have high conductivity, as in metal, since the substrates themselves would act as the electrodes that transmit the RF field, and the adhesive would act as the dielectric between them through which the electric field would develop. Structural epoxies, like most polymers, are not conductive; however, as the total loading of carbon fibers increases, so does conductivity<sup>25</sup>. If the conductivity of a composite carbon fiber/epoxy is high enough, it could act as an electrode, similar to metal, and direct contact RF bonding could be employed. Structural epoxies can be susceptible to thermal degradation and deformation, so the ability to selectively heat only the adhesive could prove very useful.

The adhesive used in this experiment was Dow BETAFORCE™ 2850-S, a 2-part polyurethane adhesive with ~10 wt% carbon black when mixed. RF energy at 30 MHz and ~5 W was applied for 25 minutes, to target a temperature of 80°C. The thermal data from this test can be seen in **Figure 14**. The carbon fiber-epoxy composite coupon heated to 34°C, barely above room temperature, due either to conduction from the heated section of adhesive or to resistive losses in the carbon fiber network. The adhesive volume was successfully heated to 80°C in 28 seconds, and roughly maintained that temperature for

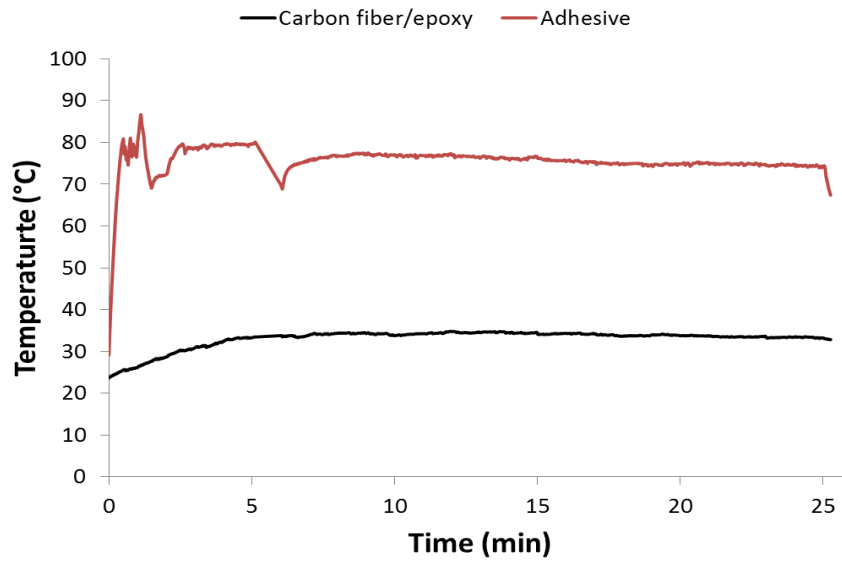


**Figure 14** - Thermal data for the carbon fiber/epoxy composite coupon and carbon black-loaded adhesive during cure

the entire 25 minutes; electrical interference from the RF signal generator caused technical difficulties with the FLIR imaging software around the 5-minute mark, resulting in the loss of one minute of thermal data. Throughout the cure, the average  $\Delta T$  between the adhesive and the composite epoxy was  $43.8^{\circ}\text{C}$ . The heating in the composite epoxy was caused by the Joule heating effect of applied electric current, while the heating in the adhesive was caused by RF. If a less resistive structural material were used, as in the case of bonding metals, resistive heating losses in the substrate would be lower, and more RF power would be applied to the adhesive. Theoretically, at a sufficiently low loading of carbon fiber, the epoxy substrate could cease to be an effective conductor of RF energy, losing more energy to Joule heating than it applies to the adhesive; however, in our samples, we found them to be sufficient conductors for use in direct-contact RF application.

## 4. CONCLUSION

### 4.1. Conclusion

This technology represents a substantial improvement over conventional heating methods. The most common device used in industrial heating, a convection heating oven, has a few issues that this technology directly solves. The first is that convection heating is indiscriminate: it will heat anything and everything inside the oven cavity. This heating happens from the outside in; if the part to be heated is covered by any kind of coating, or is located in the middle of some large assembly, the outermost structures must be heated up first. This means that if any part of an assembly needs to be oven-heated at any part in its processing, all the parts of the assembly must be oven-safe, experiencing neither deformation nor degradation when heated to the desired temperature. Another problem is how slowly ovens work. Ovens are often made with heating coils that can be maintained at a specified temperature, which then warm the air around them in an enclosed, insulated box. The air slowly equilibrates to the temperature of the heating coil, and the warm air heats the part inside the oven. The heat from the air then penetrates into the part, warming the outermost material first, and the part slowly equilibrates to the temperature of the air. This time-consuming process is tedious in an industrial manufacturing setting, where speed is almost universally desirable. Both of these issues can be solved with RF heating with carbon nanoparticles. The heating in the system can be localized just to wherever there are nanoparticles, and the heating response to the RF field is instant. Nanoparticle

loading levels and RF power can both be tuned to give higher or lower heating rates. Overall, this technology is much more precise and rapid than convection heating.

Another popular industrial heating method is infrared heating, usually accomplished with IR lamps. Infrared heating relies on radiant heating, where energy is directly transmitted to the target via electromagnetic waves. Infrared heating is often faster and more efficient than oven heating, but still suffers some similar problems. IR lamps heat somewhat indiscriminately; they can be sized to apply heat only to a specific surface area, but the heat still has to penetrate into the innermost structure, heating everything it passes through on its way. Because of this, heating with IR lamps is also slower than RF heating. With an appropriately designed applicator, RF heating could be applied in almost the exact same way as an IR lamp, but with better and quicker results.

Now that the technology has been demonstrated, the next challenge is moving toward actual application in industrial manufacturing. This heating method requires the mixing of carbon nanoparticles directly into the desired adhesive. For some polymer adhesives, this may not be an issue; carbon black is already a popular additive in plastics, paints, and coatings as a pigment or a reinforcing filler<sup>26</sup>. However, for many adhesives, adding carbon black or carbon nanotubes would require another step in the manufacturing process, a modification that may or may not be made easily. In addition, carbon nanotubes are still under investigation as a potential threat to human health<sup>27</sup> or the environment<sup>28</sup>, causing some companies to be wary of widespread adoption of nanotube usage. In addition, creating an RF applicator to fit a specific manufacturing process presents a design challenge. The applicator used in our experiments is a simple coplanar plate

capacitor on a flat plane, and the sample to be cured was a simple lap joint. However, actual manufactured parts have the potential to be much more complex, both in shape and size. The RF applicator would have to be a custom-created part for every bond geometry, and the resonant frequency of each applicator would have to be determined.

Though the thermal response of carbon nanomaterials to microwaves has been known and studied for years, and though nanomaterials (including carbon nanotubes and carbon black) have become popular fillers in heat-curing thermoset adhesives, the application of carbon nanoparticles as local heaters in RF fields is a promising, novel technology. Our group will continue to study this phenomenon, including exploring new potential RF susceptors, new applicator designs, and the ability to more precisely control resonant frequency.

## REFERENCES

- (1) Geyer, R.; Jambeck, J. R.; Law, K. L. Production, use, and fate of all plastics ever made. *Science Advances* **2017**, *3*, e1700782.
- (2) Vaia, R. A.; Wagner, H. D. Framework for nanocomposites. *Materials Today* **2004**, *7*, 32-37.
- (3) Green, M. J.; Behabtu, N.; Pasquali, M.; Adams, W. W. Nanotubes as polymers. *Polymer* **2009**, *50*, 4979-4997.
- (4) Affdl, J. C. H.; Kardos, J. L. The Halpin-Tsai equations: A review. *Polymer Engineering & Science* **1976**, *16*, 344-352.
- (5) Benítez, R.; Fuentes, A.; Lozano, K. Effects of microwave assisted heating of carbon nanofiber reinforced high density polyethylene. *Journal of Materials Processing Technology* **2007**, *190*, 324-331.
- (6) Gannon, C. J.; Cherukuri, P.; Yakobson, B. I.; Cognet, L.; Kanzius, J. S.; Kittrell, C.; Weisman, R. B.; Pasquali, M.; Schmidt, H. K.; Smalley, R. E.; Curley, S. A. Carbon nanotube-enhanced thermal destruction of cancer cells in a noninvasive radiofrequency field. *Cancer* **2007**, *110*, 2654-2665.
- (7) Higginbotham, A. L.; Moloney, P. G.; Waid, M. C.; Duque, J. G.; Kittrell, C.; Schmidt, H. K.; Stephenson, J. J.; Arepalli, S.; Yowell, L. L.; Tour, J. M. Carbon nanotube composite curing through absorption of microwave radiation. *Composites Science and Technology* **2008**, *68*, 3087-3092.
- (8) Paton, K. R.; Windle, A. H. Efficient microwave energy absorption by carbon nanotubes. *Carbon* **2008**, *46*, 1935-1941.
- (9) Mashal, A.; Sitharaman, B.; Li, X.; Avti, P. K.; Sahakian, A. V.; Booske, J. H.; Hagness, S. C. Toward Carbon-Nanotube-Based Theranostic Agents for Microwave Detection and Treatment of Breast Cancer: Enhanced Dielectric and Heating Response of Tissue-Mimicking Materials. *IEEE Transactions on Biomedical Engineering* **2010**, *57*, 1831-1834.
- (10) Irin, F.; Shrestha, B.; Cañas, J. E.; Saed, M. A.; Green, M. J. Detection of carbon nanotubes in biological samples through microwave-induced heating. *Carbon* **2012**, *50*, 4441-4449.
- (11) Zhou, X.; Shen, L.; Li, L.; Zhou, S.; Huang, T.; Hu, C.; Pan, W.; Jing, X.; Sun, J.; Gao, L.; Huang, Q. Microwave sintering carbon nanotube/Ni<sub>0.5</sub>Zn<sub>0.5</sub>Fe<sub>2</sub>O<sub>4</sub> composites and their electromagnetic performance. *Journal of the European Ceramic Society* **2013**, *33*, 2119-2126.

- (12) Liang, J.; Wang, Y.; Huang, Y.; Ma, Y.; Liu, Z.; Cai, J.; Zhang, C.; Gao, H.; Chen, Y. Electromagnetic interference shielding of graphene/epoxy composites. *Carbon* **2009**, *47*, 922-925.
- (13) Yang, Y.; Gupta, M. C.; Dudley, K. L.; Lawrence, R. W. Novel Carbon Nanotube–Polystyrene Foam Composites for Electromagnetic Interference Shielding. *Nano Letters* **2005**, *5*, 2131-2134.
- (14) Zhao, T.; Ji, X.; Jin, W.; Guo, S.; Zhao, H.; Yang, W.; Wang, X.; Xiong, C.; Dang, A.; Li, H.; Li, T.; Shang, S.; Zhou, Z. Electromagnetic wave absorbing properties of aligned amorphous carbon nanotube/BaFe<sub>12</sub>O<sub>19</sub> nanorod composite. *Journal of Alloys and Compounds* **2017**, *703*, 424-430.
- (15) Menéndez, J. A.; Arenillas, A.; Fidalgo, B.; Fernández, Y.; Zubizarreta, L.; Calvo, E. G.; Bermúdez, J. M. Microwave heating processes involving carbon materials. *Fuel Processing Technology* **2010**, *91*, 1-8.
- (16) Rigosi, A. F.; Glavin, N. R.; Liu, C.-I.; Yang, Y.; Obrzut, J.; Hill, H. M.; Hu, J.; Lee, H.-Y.; Hight Walker, A. R.; Richter, C. A.; Elmquist, R. E.; Newell, D. B. Preservation of Surface Conductivity and Dielectric Loss Tangent in Large-Scale, Encapsulated Epitaxial Graphene Measured by Noncontact Microwave Cavity Perturbations. *Small* **2017**, *13*, 1700452.
- (17) Hotta, M.; Hayashi, M.; Lanagan, M. T.; Agrawal, D. K.; Nagata, K. Complex Permittivity of Graphite, Carbon Black and Coal Powders in the Ranges of X-band Frequencies (8.2 to 12.4 GHz) and between 1 and 10 GHz. *ISIJ International* **2011**, *51*, 1766-1772.
- (18) Sweeney, C. B.; Lackey, B. A.; Pospisil, M. J.; Achee, T. C.; Hicks, V. K.; Moran, A. G.; Teipel, B. R.; Saed, M. A.; Green, M. J. Welding of 3D-printed carbon nanotube–polymer composites by locally induced microwave heating. *Science Advances* **2017**, *3*, e1700262.
- (19) Sweeney, C. B.; Moran, A. G.; Gruener, J. T.; Strasser, A. M.; Pospisil, M. J.; Saed, M. A.; Green, M. J. Radio Frequency Heating of Carbon Nanotube Composite Materials. *ACS Applied Materials & Interfaces* **2018**, *10*, 27252-27259.
- (20) Microwaves, Radio Waves, and Other Types of Radiofrequency Radiation. <https://www.cancer.org/cancer/cancer-causes/radiation-exposure/radiofrequency-radiation.html>.
- (21) Blythe, A. R. Electrical resistivity measurements of polymer materials. *Polymer Testing* **1984**, *4*, 195-209.

- (22) Lide, D. R.: *CRC handbook of chemistry and physics : a ready-reference book of chemical and physical data*; 79th ed. ed.; CRC Press: London, 1998. pp. approximately 2000 pages in various pagings : tables ; 26 cm.
- (23) Michaels, R.: Q&A: How to properly cure an epoxy for the aerospace industry. MasterBond®, 2014.
- (24) Mehdizadeh, M.: Chapter 2 - Fundamentals of Field Applicators and Probes at RF and Microwave Frequencies. In *Microwave/RF Applicators and Probes for Material Heating, Sensing, and Plasma Generation*; Mehdizadeh, M., Ed.; William Andrew Publishing: Boston, 2010; pp 35-66.
- (25) Jawad, S. A.; Ahmad, M.; Ramadin, Y.; Zihlif, A.; Paesano, A.; Martuscelli, E.; Ragosta, G. Electrical properties of laminated epoxy-carbon fiber composite. *Polymer International* **1993**, 32, 23-31.
- (26) Ceresana. *Carbon Black Market Report* for Ceresana: Ceresana Market Research2018.
- (27) Chernova, T.; Murphy, F. A.; Galavotti, S.; Sun, X.-M.; Powley, I. R.; Grosso, S.; Schinwald, A.; Zacarias-Cabeza, J.; Dudek, K. M.; Dinsdale, D.; Le Quesne, J.; Bennett, J.; Nakas, A.; Greaves, P.; Poland, C. A.; Donaldson, K.; Bushell, M.; Willis, A. E.; MacFarlane, M. Long-Fiber Carbon Nanotubes Replicate Asbestos-Induced Mesothelioma with Disruption of the Tumor Suppressor Gene Cdkn2a (Ink4a/Arf). *Current biology : CB* **2017**, 27, 3302-3314.e3306.
- (28) Tejral, G.; Panyala, N. R.; Havel, J. Carbon nanotubes: toxicological impact on human health and environment. *Journal of Applied Biomedicine (De Gruyter Open)* **2009**, 7, 1-13.